ORIGINAL ARTICLE

The influence of geological events on the endemism of East Asian birds studied through comparative phylogeography

Yanhua Qu[1], Gang Song[1], Bin Gao[1], Qing Quan[1], Per G. P. Ericson[2] and Fumin Lei[1]*

[1]Key Laboratory of Zoological Systematics and Evolution, Institute of Zoology, Chinese Academy of Sciences, Beijing 100101, China, [2]Department of Vertebrate Zoology, Swedish Museum of Natural History, PO Box 50007, SE-10405 Stockholm, Sweden

ABSTRACT

Aim East Asia is known for its exceptionally high biological diversity and endemism. Various geological and climatic events during the Pliocene and Pleistocene have been invoked to explain this high endemism, and these processes have had different impacts on different organisms. Herein, we investigate the relative role of these historical processes in the genetic evidence for endemism of intraspecific lineages of two East Asian species: the grey-cheeked fulvetta (*Alcippe morrisonia*) and the red-headed tree babbler (*Stachyridopsis ruficeps*).

Location East Asia.

Methods We studied the genetic structure based on mitochondrial and nuclear DNA and evaluated the phylogeographical lineages using coalescent species tree approaches. The influences of different historical processes on diversification among phylogeographical lineages were analysed using coalescent models. We tested correlations between ecological divergence and phylogeographical splits.

Results The genetic structure analysis and species tree estimation revealed three deeply divergent lineages within both species. One lineage is endemic to the mountains of Southwest China and the other to Taiwan. Coalescent simulations suggested that lineage diversification mostly occurred during the late Pliocene. Within this time frame, uplift of the mountains of Southwest China and formation of the island of Taiwan are geological events consistent with the geographical isolation and ecological niche divergence of these phylogeographical lineages.

Main conclusions Our results suggest that the main driver of avian endemism in East Asia was the formation of new montane and island habitats following the uplift of the mountains of Southwest China and formation of the island of Taiwan in the Pliocene. However, the populations in the two regions were affected differently by the climatic oscillations during the Pleistocene. The mountains of Southwest China were climatically stable during glaciations, allowing populations to persist throughout the Pleistocene and maintain their genetic uniqueness. In contrast, glaciations resulted in lowered sea levels, allowing dispersal between the island of Taiwan and mainland China, thus obscuring the genetic endemism of the Taiwanese populations.

Keywords
Alcippe morrisonia, allopatric divergence, birds, East Asia, ecological vicariance, genetic endemism, genetic diversification, South China, *Stachyridopsis ruficeps*, Taiwan.

*Correspondence: Fumin Lei, Institute of Zoology, Chinese Academy of Sciences, No. 1 Beichen West Road, Chaoyang District, Beijing 100101, China.
E-mail: leifm@ioz.ac.cn

INTRODUCTION

South China is a biodiversity hotspot in East Asia, harbouring two particular areas of endemism for birds and other organisms: the mountains of Southwest China and the island of Taiwan (Stattersfield *et al.*, 1998; Lei *et al.*, 2003a,b). The high degree of endemism in these areas may reflect their dramatic geological history and the glacial oscillations that occurred during the Pliocene and Pleistocene. Tectonic activities in South China included tectonic uplift in the late Miocene and Pliocene, resulting in high mountain systems, such as the eastern Himalayas, the mountains of Southwest China and the Qinling Mountains (Quade *et al.*, 1989; Webb & Bartlein, 1992). The formation of the Taiwan Strait was also a consequence of tectonic activity and led to the isolation of the island of Taiwan, which was later reconnected to the mainland by a land bridge during periods of low sea levels in the Pleistocene (Voris, 2000; Yu *et al.*, 2000). The topographically complex landscape formed in the Pliocene by the mountain ridges and large islands probably caused populations to be geographically isolated, subsequently leading to their diversification and speciation, e.g. deep divergently phylogenetic lineages were observed within the mountain systems and ecoregions of Southwest China's mountainous region (Päckert *et al.*, 2012; Qu *et al.*, 2014), and many endemic species, subspecies and isolated phylogenetic lineages were found on the island of Taiwan (Lei *et al.*, 2003a,b). The glaciations that took place during the Pleistocene were another likely contributor to diversification in East Asia. During these glaciations, the area of suitable habitats retreated, and populations contracted to few environmentally stable refugia, where their long-term isolation may have driven genetic divergence (Li *et al.*, 2009; Lei *et al.*, 2014). The changing topography and environment during the Pliocene and Pleistocene in East Asia may have caused ecological divergence between populations adapting to the new environments. This, in turn, may have worked in concert with isolation to lead to the formation of new lineages and contributed further to the genetic diversification of East Asian organisms (Liu *et al.*, 2012; Päckert *et al.*, 2012).

The grey-cheeked fulvetta, *Alcippe morrisonia* Swinhoe, 1863, and the red-headed tree babbler, *Stachyridopsis ruficeps* (Blyth, 1847), are two small species of babblers (Aves, Timaliidae) that are commonly found in East Asia, mainly in South China. Both species inhabit broadleaf evergreen forests from 200 m a.s.l. to 2500 m a.s.l. Previous mitochondrial DNA (mtDNA) analyses identified exceptionally high intraspecific variation between seven lineages (phylogroups) of *A. morrisonia* and six of *S. ruficeps* (Song *et al.*, 2009; Liu *et al.*, 2012). The estimated divergence times between these genetic lineages span from the Miocene to the late Pleistocene in both species. It is unlikely that a single geological process can be invoked to explain all of the known diversity of *A. morrisonia* and *S. ruficeps*. We postulate that three factors have driven genetic diversification in *A. morrisonia* and

S. ruficeps: (1) the formation of mountain ranges and large islands during the Pliocene caused geographical isolation; (2) Pleistocene glaciations isolated populations into pockets of suitable habitats; and (3) the opening up of new niches following changes in the environment since the Pliocene also led to ecological divergence among phylogeographical lineages. To evaluate the relative importance of these three factors in explaining the genetic structure observed today in *A. morrisonia* and *S. ruficeps*, we employed a combination of multilocus comparative phylogeography, approximate Bayesian computation (ABC) simulated coalescent model, and ecological vicariance analysis. We specifically sought to determine whether phylogenetic trees based on multiple nuclear gene loci would reveal intraspecific patterns similar to those previously reported based on mtDNA (Song *et al.*, 2009; Liu *et al.*, 2012).

MATERIALS AND METHODS

Sampling and sequence data

Tissue and blood samples were obtained from 41 individuals of *A. morrisonia* from 19 localities and 34 individuals of *S. ruficeps* from 20 localities (Fig. 1 and see Appendix S1 in Supporting Information). Samples were preserved in 100% ethanol and kept in bird specimen collection of the National Zoological Museum, Institute of Zoology. These samples were collected across the distribution ranges of the species in South China. Five to seven representatives from each of the previously identified mtDNA lineages were included in the analyses.

DNA was extracted from tissue and blood samples using the DNeasy Tissue kit (Qiagen, Beijing, China). We amplified and sequenced 10 single-copy nuclear DNA (nDNA) loci using primers specifically designed for *A. morrisonia* and *S. ruficeps*, respectively (Gao *et al.*, 2012). For comparison, we also used a mtDNA fragment combining the cytochrome *b* and COI genes (Song *et al.*, 2009; Liu *et al.*, 2012).

Phylogenetic and population structure analyses

We reconstructed phylogenetic trees for mtDNA sequences using BEAST 1.7.1 (Drummond & Rambaut, 2007). We used the substitution model GTR+G+I for both species based on the Akaike information criterion (AIC) in MODELTEST 3.7 (Posada & Crandall, 1998). A constant model was used in all BEAST runs. For each species, two independent analyses were run for 100 million generations, and trees were sampled every 1000 generations. Convergence to the posterior distributions of parameter estimates was examined in TRACER 1.5 (Rambaut & Drummond, 2007), and the burn-in was set to 25,000 trees (25% of all sampling trees). A maximum credibility tree representing the maximum posterior topology was calculated after removing trees sampled during the burn-in phase.
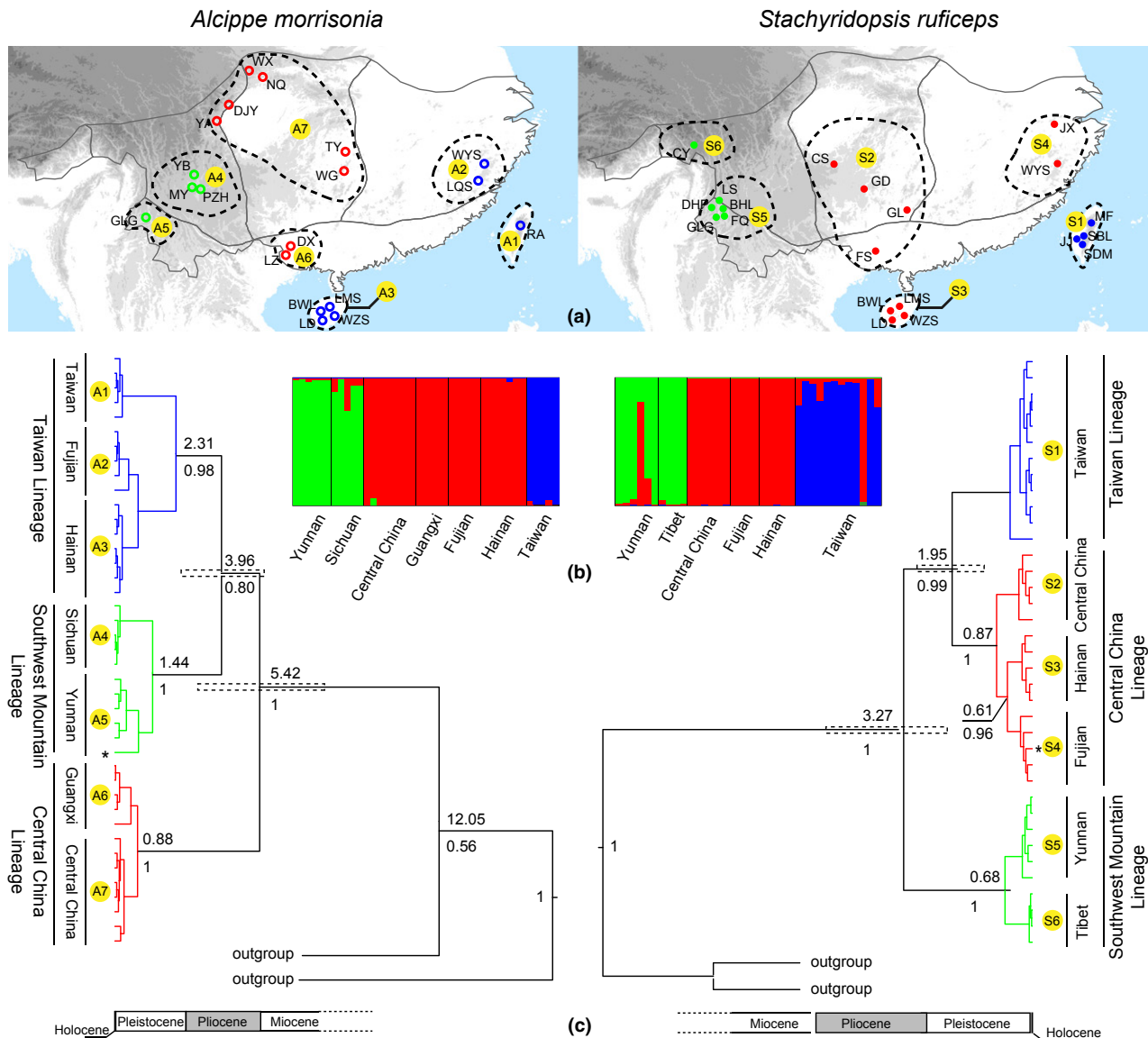
Figure 1 Sampling sites, mitochondrial DNA phylogenetic trees, and genetic structure of the nuclear DNA of *Alcippe morrisonia* and *Stachyridopsis ruficeps*. Green indicates individuals belonging to the Southwest Mountain lineages; blue indicates the Taiwan lineages; and red indicates the Central China lineages. Broken line polygons show the geographical distributions of mitochondrial lineages as reconstructed in previous studies (Song *et al.*, 2009; Liu *et al.*, 2012) and numbers in yellow circles identify individual phylogeographical lineages. (a) Sampling sites for the two species of babblers; open circles represent *A. morrisonia*, and filled circles represent *S. ruficeps*; (b) nuclear genetic structure inferred through Bayesian based cluster analysis implemented in STRUCTURE; and (c) maximum clade credibility tree estimated using BEAST for the mitochondrial gene. Values below branches indicate Bayesian posterior probability, and values above branches represent the divergence-time estimates if we assumed a conventional mutation rate of 0.01 substitutions per site per million years for the avian mitochondrial gene.

The individual gene trees were reconstructed for nDNA loci using MrBayes 3.2 (Ronquist & Huelsenbeck, 2003). Two independent runs were conducted with trees sampled every 100 generations for 1×10^7 generations. The first 25% of the generations were regarded as belonging to the burn-in phase and discarded. Posterior probabilities were estimated for the subsequent generations. Furthermore, we identified genetic structure in 10 nuclear loci using STRUCTURE 2.3.2 (Pritchard *et al.*, 2000) with a burn-in of 1×10^{-6} and 1×10^{-7} iterations, prior population information and the

admixture model. We conducted 10 replicate runs for each value of K (the number of populations). The number of populations was set to 1 to 6 for *S. ruficeps* and 1 to 7 for *A. morrisonia* to cover the numbers of main lineages that could be identified in the mtDNA trees (see Results). The most likely value of K was identified using the maximal value of Pr(X/K), which is typically used for STRUCTURE analysis, and ΔK, based on the rate of change in the posterior probability of data between successive K values (Evanno *et al.*, 2005).

Coalescent species tree estimation

Three coalescent-based approaches were employed to estimate species trees from the gene trees. First, we applied BEST 2.3.1 (Liu & Pearl, 2007), as outlined in Carstens & Dewey (2010), wherein likelihood scores were calculated and compared for species trees generated under three species delimitation hypotheses. Because BEST requires a priori assignment of individuals to species categories, we performed a set of analyses in which individuals were assigned to different groups as postulated by the three hypotheses. The first hypothesis stated that all individuals belong to the same species (one-species tree, i.e. the traditional taxonomical treatment of these species). The second hypothesis stated that *A. morrisonia* and *S. ruficeps* should each be divided into three species (three-species tree), which may be inferred from the structure detected in their nDNA and from the three major lineages of mtDNA observed in both species (see Results). The third hypothesis stated that there were multiple mitochondrial groups in the two species (seven-species tree for *A. morrisonia* and six-species tree for *S. ruficeps*). BEST was used to estimate the likelihood scores for the species trees constructed under the three hypotheses, and the analyses were conducted with duplicate runs including 2×10^9 generations, a sampling frequency of 1000 generations and one coupled Markov chain. The prior settings included an inverse gamma (3.0, 0.003) and a uniform mutation prior (0.5, 1.5), and the analyses were conducted using a partitioned model that matched that selected for each locus (Table 1). The

natural logarithm Bayes factor (ln BF) was calculated as measure of support for each species delimitation hypothesis using TRACER. In accordance with Kass & Raftery (1995), we considered $2 \times \ln BF$ (H_1 vs. H_2) > 10 as decisive support for hypothesis H_1 versus hypothesis H_2. Likewise, $2 \times \ln BF$ (H_1 vs. H_2) > −10 was considered as decisive evidence against hypothesis H_1 versus H_2.

Second, species delimitation hypotheses were tested using the program BPP 2.0 (Yang & Rannala, 2010) and we ran the reversible-jump Markov chain Monte Carlo (rjMCMC) analyses for 500,000 generations (sampling interval of five) with a burn-in phase of 100,000. We set two different combinations of priors. The first combination assumed relatively large ancestral population size and deep divergence: $\theta \sim G$ (1, 10) and $\tau_0 \sim G$ (1, 10). The second combination of priors assumed relatively small ancestral population size and shallow divergence: $\theta \sim G$ (2, 2000) and $\tau_0 \sim G$ (2, 2000). The other divergence-time parameters were assigned to be the Dirichlet prior (Yang & Rannala, 2010). Each analysis was run twice with different starting seeds to check consistency.

Third, we employed the gene tree simulation method using MESQUITE 2.7.2 (Maddison & Maddison, 2009). For both the mitochondrial and nuclear gene trees, deep coalescent events (DC) and Slatkin's S score were calculated and applied as metrics for assessing their fit to the species trees. In the coalescent simulations, we assumed a generation time of 2 years (Cheng *et al.*, 1982). The mean population mutation parameters θ, where θ is the product of effective population size (N_e) and mutation rate μ per site, and their lower

Table 1 Nucleotide polymorphism of different genes and nucleotide evolution model of the two babblers, *Alcippe morrisonia* and *Stachyridopsis ruficeps*.

Species	Genes	Gene types	n	Length (bp)	S	π	Nucleotide evolution model
Alcippe morrisonia	Cyt *b* and COI	mtDNA	41	1236	203	0.054	GTR+I+G
	Am19	nDNA	41	1109	19	0.0026	GTR
	Am39	nDNA	40	788	34	0.0041	GTR+I
	Am44	nDNA	41	848	129	0.0211	GTR+I+G
	Am48	nDNA	36	918	71	0.0138	GTR+I+G
	Am54	nDNA	39	987	66	0.0111	GTR+I+G
	Am83	nDNA	40	679	77	0.0151	HKY+G
	Am90	nDNA	40	738	86	0.0140	GTR+I
	Am91	nDNA	40	1093	65	0.0080	GTR+I+G
	Am102	nDNA	39	931	81	0.0121	GTR+I+G
	Am179	nDNA	40	807	63	0.0058	HKY+G
Stachyridopsis ruficeps	Cyt *b* and COI	mtDNA	37	2175	212	0.0298	GTR+I+G
	Su02	nDNA	32	1213	54	0.0075	GTR+I+G
	Su04	nDNA	36	1063	46	0.0050	HKY+I+G
	Su06	nDNA	31	1194	57	0.0077	GTR+I+G
	Su07	nDNA	26	1163	59	0.0088	GTR+I+G
	Su11	nDNA	37	1008	98	0.0153	GTR+I+G
	Su25	nDNA	35	1154	37	0.0203	HKY+I+G
	Su42	nDNA	26	1040	83	0.0188	GTR+I+G
	Su43	nDNA	37	827	16	0.0030	HKY+I
	Su47	nDNA	31	978	76	0.0115	GTR+I+G
	Su84	nDNA	28	1243	70	0.0107	HKY+I

n, sampling size; S, number of segregating sites; π, nucleotide divergence.

and upper bounds of the 95% confidence intervals, were estimated for mtDNA using FLUCTUATE 1.4 (Kuhner *et al.*, 1998) and scaled to *Ne* using a mutation rate of 1×10^{-8} per year. Divergence times, which were converted to numbers of generations, were set to be the lower and upper bounds of the ABC estimated divergence times (Table 2). Under each species delimitation model, a set of 1000 gene trees was generated for each value of the effective population sizes. We calculated the DC and Slatkin's *S* scores for the simulated gene trees for the mitochondrial and nuclear datasets, respectively, and compared them with those of the observed mitochondrial and nuclear gene trees.

The relative roles of Pliocene tectonic events and Pleistocene glaciations in the current genetic structure

The time range of the major diversification events in *A. morrisonia* and *S. ruficeps* has previously been estimated based on mtDNA (Song *et al.*, 2009; Liu *et al.*, 2012). However, the wide range of the obtained time estimates has made it impossible to evaluate whether the diversification patterns observed in the two species of babblers resulted from geological events in the Pliocene or climatic factors in the Pleistocene. To obtain robust data on the divergence of these species, and, thus, on their biogeography, we formulated two evolutionary hypotheses, which were then analysed using DIYABC 1.0.4.46 (Cornuet *et al.*, 2008). The two hypotheses focus on the diversification among the three phylogenetic lineages inferred from the coalescent species trees (see Results). In the first, we hypothesized that late Pliocene divergence occurred as the uplift of the mountains of Southwest China and the formation of the island of Taiwan. In the second, we hypothesized more recent diversification of the two species as a result of the repeated isolation of populations in various glacial refugia during the Pleistocene (Appendix S2, H_1 and H_2).

The two models were tested using DIYABC, and summary statistics were calculated for mtDNA and nDNA, which included the mean and variance of pairwise differences for a single population, the mean of pairwise differences (*B*) and F_{ST} between two populations. Because of computational constraints, we had to base the summary statistics on one mitochondrial and three nuclear loci (*A. morrisonia*, Am48, Am54 and Am83; *S. ruficeps*, Su4, Su47 and Su84). These nuclear loci were selected because they showed higher genetic variation among three lineages than other loci, based on genetic distance (Table 1) and topological structures of gene trees (Appendix S3). Prior distributions of the demographic parameters were defined to maximize the genetic parameters of the studied species (Table 2). Under both hypotheses, we set the lower and upper bounds of the Pliocene (2.59–5.3 Ma) and the Pleistocene (0.01–2.59 Ma) as the minimum and maximum divergence time among the three lineages. We applied HKY models for all loci. For each hypothesis, we used 1×10^6 simulated data points to build a reference table. The posterior probabilities of the two competing hypotheses were computed via logistic regression employing 1% of the simulated datasets that were closest to the observed data (using the Euclidean distance between each simulated and observed dataset). For each comparison, the preferred hypothesis is the one with the highest posterior probability.

Table 2 Prior distribution parameters describing the each set of hypotheses investigated for *Alcippe morrisonia* and *Stachyridopsis ruficeps*, and posterior probability distribution of the demographic parameters obtained for the most supported scenario in approximate Bayesian computation (ABC) analyses. *N*, effective population size; *Na*, effective population size of the ancestral populations; T_1, the divergence time under the Pliocene divergence hypothesis; T_2, the divergence time under the Pleistocene divergence hypothesis.

Parameters	Prior distribution (min–max)	Posterior distribution (mean ± 95% HPD)
Alcippe morrisonia		
Effective population size		
$N_{Southwest\_Mountains}$	Uniform (20000–2000000)	9.80×10^5 (4.17×10^5–1.51×10^6)
$N_{Central\_China}$	Uniform (20000–2000000)	1.40×10^6 (0.66×10^5–1.94×10^6)
N_{Taiwan}	Uniform (20000–2000000)	3.42×10^5 (4.61×10^4–1.15×10^6)
Na	Uniform (200–200000)	
Time of divergence		
T_1_Pliocene	Uniform (1.8–5.2 Ma)	3.64 (2.64–4.8 Ma)
T_2_Pleistocene	Uniform (0.1–1.8 Ma)	2.58 (2.56–4.68 Ma)
Stachyridopsis ruficeps		
Effective population size		
$N_{Southwest\_Mountains}$	Uniform (20000–2000000)	5.73×10^5 (1.39×10^5–1.11×10^6)
$N_{Central\_China}$	Uniform (20000–2000000)	1.39×10^6 (0.83×10^5–1.91×10^6)
N_{Taiwan}	Uniform (20000–2000000)	7.02×10^5 (2.40×10^5–1.62×10^6)
Na	Uniform (200–200000)	
Time of divergence		
T_1_Pliocene	Uniform (1.8–5.2 Ma)	3.98 (2.72–4.92 Ma)
T_2_Pleistocene	Uniform (0.1–1.8 Ma)	3.10 (2.44–4.36 Ma)

HPD, highest posterior density interval.

Ecological vicariance analyses

We used two approaches to test ecological divergence among three phylogenetic lineages of two babblers (coalescent species trees, see Results). First, we used ENMTOOLS (Warren *et al.*, 2008) to calculate Schoener's *D* (Schoener, 1968) and Warren *et al.*'s *I* statistic (Warren *et al.*, 2008). These measures assign a numerical value that ranges from zero (no niche overlap) to one (identical niches), and provide an indication of niche similarity for that comparison. We performed the identity and background randomization tests and calculated the observed *D* and *I* values and simulated distributions of *D* and *I* using 100 replicates for all pairwise comparisons.

Second, we tested the correlations between the ecological divergences and the phylogenetic splits using spatial evolutionary and ecological vicariance analysis (SEEVA; Struwe *et al.*, 2011). SEEVA assumes that if shifts in ecological adaptations are responsible for the split of an old lineage into two new lineages, it should be reflected in ecological divergence between the new lineages. The probability of this expectation can be estimated statistically using the null hypothesis that ecological separations and phylogenetic divergences should be independent from each other. We extracted 10 environmental variables for each sampling site in ArcGIS (ESRI, Redlands, CA, USA), and primary GIS data layers for temperature and precipitation were obtained from WorldClim v. 1.4 (http://www.worldclim.org/; Hijmans *et al.*, 2005). Quantitative variables (temperature, elevation and precipitation) were scored as ordered, continuous data, while the qualitative variables (vegetation type) were treated as non-ordered, categorical data. We divided these variables into four states according to the default setting in SEEVA (four quartile classes in quantitative variables and four state frequencies by combining related types). We investigated the correlations between ecological shifts and the phylogenetic splits using Fisher's exact tests and divergence indices (*D*).

RESULTS

Genetic polymorphism

For mtDNA, we obtained 1236 bp and 2175 bp combined for the cytochrome *b* and COI genes for *A. morrisonia* and *S. ruficeps*, respectively. For nDNA, we amplified and sequenced 10 loci with lengths from 679 bp to 1236 bp and 827 bp to 1243 bp for *A. morrisonia* and *S. ruficeps*, respectively. The observed genetic polymorphism in the mitochondrial genes was generally higher than in the nuclear genes (Table 1).

Phylogenetic and population structure analyses

The mitochondrial gene analyses revealed distinct geographical structure in both species (Fig. 1), and several groups of sampling localities could be distinguished. In *A. morrisonia*, seven such locality groups (Fujian, Hainan, Taiwan, Yunnan, Sichuan, Central China and Guangxi) could be identified, and in *S. ruficpes*, six locality groups (Fujian, Hainan, Taiwan, Yunnan, Tibet and Central China) were observed. In both species, the mitochondrial gene analyses grouped the samples into reciprocally monophyletic lineages that corresponded roughly to the different geographical regions. In *A. morrisonia*, three such major lineages were identified: (1) a Taiwan lineage (Taiwan, Hainan and Fujian locality groups); (2) a lineage from the mountains of Southwest China (Southwest Mountain lineage; Sichuan and Yunnan locality groups); and (3) a Central China lineage (Guangxi and Central China locality groups). The phylogeographical structure in *S. ruficeps* closely resembled that of *A. morrisonia* but differs in the relative position of the Hannan and Fujian locality groups (Fig. 1). The *S. ruficeps* samples were grouped into the same three reciprocally monophyletic lineages: (1) a Taiwan lineage (Taiwan locality group); (2) a Southwest Mountain lineage (Yunnan and Tibet locality groups); and (3) a Central China lineage (Central China, Hainan and Fujian locality groups).

The phylogenetic divergence in nuclear gene trees was more distinct in S. *ruficeps* than in *A. morrisonia* because the three-lineage pattern revealed by mtDNA trees was observed in most gene trees of S. *ruficpes*, but not in those of *A. morrisonia* (Appendix S3). STRUCTURE analyses of all the nuclear genes identified similar three-lineage divisions in both S. *ruficeps* and *A. morrisonia*, although the samples from the island of Taiwan in *A. morrisonia* formed an independent lineage in nuclear gene structure, rather than being clustered with Hainan and Fujian locality groups as in the mtDNA tree (Fig. 1).
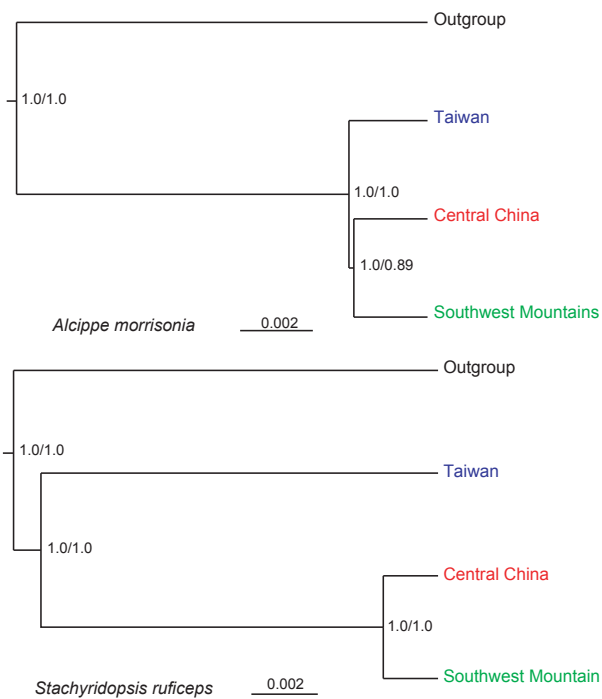
Coalescent species tree estimation

Species trees were generated using BEST under the three species delimitation hypotheses, and their likelihood scores were compared with ln BF tests. For both *A. morrisonia* and *S. ruficeps*, the trees based on the three-species hypothesis produced a higher likelihood score than those for the alternative hypotheses (Table 3), suggesting that both species may be viewed as consisting of three major genetic lineages (Fig. 2). Lineages division and the phylogenetic relationship among lineages were similar for both species. BPP species tree estimates were in agreement with BEST results with strong support (posterior = 1.0) for three-species tree in both *A. morrisonia* and *S. ruficeps* (Fig. 2). Different prior distributions for θ and τ_0 did not affect the result. The DC and Slatkin's *S* statistics for comparison between the simulated and the observed mitochondrial and nuclear gene trees also supported the three-species tree for both *A. morrisonia* and *S. ruficeps* (Table 4).

The relative roles of Pliocene tectonic events and Pleistocene glaciations in the current genetic structure

For *A. morrisonia*, ABC was unable to distinguish between the two hypotheses when mitochondrial and nuclear data were analysed together. To better understand the characteristics of

Table 3 Likelihood scores and test statistics 2 × ln Bayes factor (BF) comparisons for BEST analysis of species delimitation hypotheses in *Alcippe morrisonia* and *Stachyridopsis ruficeps*. The compared hypotheses are arranged in rows and columns, respectively, and a 2 × ln BF > 10 is considered as decisive support.

Species	Hypothesis	−ln L	2 × ln BF One-species hypothesis	Three-species hypothesis	Seven-species hypothesis
Alcippe morrisonia	One-species delimitation	−26945.53		−1100.67	672.94
	Three-species delimitation	−25856.23	1100.67		1773.6
	Seven-species delimitation	−27455.28	−672.94	−1773.6	
Stachyridopsis ruficeps	One-species delimitation	−29991.46		−610.71	1770.92
	Three-species delimitation	−29381.39	610.07		2380.98
	Seven-species delimitation	−31762.38	−1770.92	−2380.98	

Figure 2 Coalescent species tree estimated by three approaches (BEST, BPP and MESQUITE) for *Alcippe morrisonia* and *Stachyridopsis ruficeps*, respectively. The combined datasets of the mitochondrial gene and 10 nuclear genes are used. Three species different delimitation hypotheses were tested and the three-species tree hypothesis was supported for both taxa. Posterior probabilities for nodes of the three-species trees are shown above the branches (BEST/BPP). Branch lengths show divergence time unit in substitution rate per site.

each dataset, we analysed the mitochondrial and nuclear datasets separately. The results were contradictory: the nuclear dataset suggested the Pliocene divergence hypothesis to be the most likely, whereas the mitochondrial dataset supported the Pleistocene divergence hypothesis (Table 5). Considering that the Taiwan locality group clustered with the Fujian and the Hainan locality groups for the mitochondrial data, we suspected that individuals of *A. morrisonia* in Taiwan had dispersed to the Fujian region and Hainan Island during the Pleistocene (see Discussion). We therefore analysed the data under the hypothesis that the Taiwan lineage of *A. morrisonia*

diverged from the Central China lineage in the Pliocene but was admixed during the Pleistocene glaciations (Appendix S2, H_3). Indeed, the ABC result for the combined datasets supported this Pleistocene admixture hypothesis (Table 5). The posterior distributions of the demographic parameters estimated based on the combined datasets under the hypothesis of Pliocene divergence followed by admixture during the Pleistocene implied that the Taiwan lineage diverged from the other two lineages at 3.64 Ma and that the Southwest Mountain lineage and the Central China lineage diverged at 3.58 Ma (Table 2).

For *S. ruficeps*, logistic regression estimates of the posterior probabilities showed the Pliocene divergence hypothesis to be the most likely (Table 5). The posterior distributions of the demographic parameters estimated based on the best-supported hypothesis showed that the Taiwan lineage was the first to diverge from the other two lineages at 3.98 Ma and that the Southwest Mountain lineage and the Central China lineages diverged at 3.1 Ma (Table 2).

Ecological vicariance analyses

Both identity and background tests using ENMTools showed that the Schoener's D and I values for the pairwise comparisons of three phylogenetic lineages of two species were significantly lower than expected from the random distributions ($P \leq 0.01$), thus indicating that the three phylogenetic lineages of the two species were ecologically distinct lineages (Table 6).

SEEVA compared 10 environmental variables between the sister lineages for each species. In *A. morrisonia* 12 of the 20 comparisons were significant ($P \leq 0.025$ after Bonferroni correction indicated by an asterisk in Table 7), and in *S. ruficeps*, 13 of 20 comparisons were significant (Table 7). For both species, the phylogenetic splits between the Southwest Mountain lineage and the Central China lineage showed strong divergence in terms of elevation ($D = 0.95^*$ in *A. morrisonia* and $D = 0.94^*$ in *S. ruficeps*), vegetation ($D = 0.4^*$–1.0^* in *A. morrisonia* and $D = 0.88^*$–1.0^* in *S. ruficeps*), temperature ($D = 0.42^*$–0.96^* in *A. morrisonia* and $D = 0.56^*$–1^* in *S. ruficeps*), and precipitation ($D = 0.48^*$–0.94^* in *A. morrisonia* and $D = 0.48^*$–0.58^* in *S. ruficeps*). However, the split between the Taiwan and Central China lineages only showed

Table 4 Simulated deep coalescent events (DC) and Slatkin's *S* distributions for mitochondrial and nuclear gene trees in *Alcippe morrisonia* and *Stachyridopsis ruficeps*. For *S. ruficeps*, the observed DC and Slatkin's *S* values for the mitochondrial gene tree are 0 and 2, respectively, and 4 and 2 for the nuclear gene tree under the three-species hypothesis. Under the seven-species delimitation hypothesis, observed DC and Slatkin's *S* values for the mitochondrial gene tree are 3 and 6, respectively, and 10 and 10 for the nuclear gene tree. For *A. morrisonia*, the observed DC and Slatkin's *S* values for the mitochondrial gene tree are 1 and 2, respectively, and 2 and 2 for the nuclear gene tree under the three-species hypothesis. Under the seven-species delimitation hypothesis, observed DC and Slatkin's *S* values for the mitochondrial gene tree are 1 and 6, respectively, and 24 and 15 for the nuclear gene tree.

Species	Hypothesis	Gene	Time	*Ne*	DC	Slatkin's *S*
Stachyridopsis ruficeps	Three-species delimitation	Mitochondrial gene	2.5 Ma	Mean (6.0×10^5)	0–1	2
				Lower (5.3×10^5)	0–1	2
				Upper (6.7×10^5)	0–1	2
			5.0 Ma	Mean (6.0×10^5)	0	2
				Lower (5.3×10^5)	0	2
				Upper (6.7×10^5)	0	2
		Nuclear gene	2.5 Ma	Mean (2.4×10^6)	0–4	2–5
				Lower (2.1×10^6)	0–4	2–4
				Upper (2.7×10^6)	0–5	2–5
			5.0 Ma	Mean (2.4×10^6)	0–2	2–3
				Lower (2.1×10^6)	0–2	2–3
				Upper (2.7×10^6)	0–2	2–3
	Seven-species delimitation	Mitochondrial gene	2.5 Ma	Mean (6.0×10^5)	0	5
				Lower (5.3×10^5)	0	5
				Upper (6.7×10^5)	0	5
			5.0 Ma	Mean (6.0×10^5)	0	5
				Lower (5.3×10^5)	0	5
				Upper (6.7×10^5)	0	5
		Nuclear gene	2.5 Ma	Mean (2.4×10^6)	0–3	5–7
				Lower (2.1×10^6)	0–3	5–6
				Upper (2.7×10^6)	0–3	5–7
			5.0 Ma	Mean (2.4×10^6)	0–1	5
				Lower (2.1×10^6)	0–1	5
				Upper (2.7×10^6)	0–2	5
Alcippe morrisonia	Three-species delimitation	Mitochondrial gene	2.5 Ma	Mean (8.1×10^5)	0–2	2–3
				Lower (7.2×10^5)	0–1	2–3
				Upper (9.1×10^5)	0–2	2–3
			5.0 Ma	Mean (8.1×10^5)	0	2
				Lower (7.2×10^5)	0	2
				Upper (9.1×10^5)	0	2
		Nuclear gene	2.5 Ma	Mean (3.2×10^6)	0–5	2–5
				Lower (2.9×10^6)	0–5	2–5
				Upper (3.6×10^6)	0–6	2–6
			5.0 Ma	Mean (3.2×10^6)	0–3	2–5
				Lower (2.9×10^6)	0–3	2–5
				Upper (3.6×10^6)	0–4	2–6
	Seven-species delimitation	Mitochondrial gene	2.5 Ma	Mean (8.1×10^5)	0–1	6
				Lower (7.2×10^5)	0	6
				Upper (9.1×10^5)	0–1	6
			5.0 Ma	Mean (8.1×10^5)	0	6
				Lower (7.2×10^5)	0	6
				Upper (9.1×10^5)	0	6
		Nuclear gene	2.5 Ma	Mean (3.2×10^6)	0–3	6–8
				Lower (2.9×10^6)	0–3	6–9
				Upper (3.6×10^6)	0–4	6–9
			5.0 Ma	Mean (3.2×10^6)	0–1	6
				Lower (2.9×10^6)	0–1	6
				Upper (3.6×10^6)	0–2	6–7

Ne, effective population size.

slight divergence in elevation (non-significant *D* in *A. morrisonia* and *S. ruficeps*) and temperature (only one temperature variable showing significant *D* values in *A. morrisonia* and *S. ruficeps*), but showed strong divergence in the precipitation variables ($D = 0.83$* in *A. morrisonia* and $D = 0.9$* in *S. ruficeps*; Fig. 3, Table 7).

Table 5 Estimates of posterior probabilities and 95% confidence intervals for competing hypotheses for diversification time of *Stachyridopsis ruficeps* and *Alcippe morrisonia* using approximate Bayesian computation.

Species	Datasets	Hypothesis	Posterior probability
Stachyridopsis ruficeps	Combined dataset	Pliocene divergence	0.705 (0.684–0.725)
		Pleistocene divergence	0.295 (0.275–0.316)
Alcippe morrisonia	Combined dataset	Pliocene divergence with Pleistocene admixture	0.780 (0.762–0.797)
		Pliocene divergence	0.079 (0.068–0.091)
		Pleistocene divergence	0.141 (0.127–0.155)
Alcippe morrisonia	Mitochondrial dataset	Pliocene divergence	0.138 (0.129–0.146)
		Pleistocene divergence	0.862 (0.854–0.871)
	Nuclear dataset	Pliocene divergence	0.847 (0.836–0.857)
		Pleistocene divergence	0.153 (0.143–0.164)

Table 6 Tests of niche similarity in *Alcippe morrisonia* and *Stachyridopsis ruficeps* using ENMTools. Each test is followed by an assessment of statistical significance. TW, Taiwan lineage; SM, Southwest Mountain lineage; CC, Central China lineage.

	Pairwise	Identity test		Background test	
		I	D	I	D
Alcippe morrisonia	SM vs. CC	0.776**	0.460**	0.776**, **	0.460**, **
	SM vs. TW	0.685**	0.442**	0.685**, **	0.442**, **
	CC vs. TW	0.699**	0.425**	0.699**, **	0.425**, **
Stachyridopsis ruficeps	SM vs. CC	0.723**	0.478**	0.723**, n.s.	0.478**, n.s.
	SM vs. TW	0.708**	0.412**	0.708**, **	0.412**, **
	CC vs. TW	0.636**	0.345**	0.636**, **	0.345**, **

Note: Significance of background tests are given as 'the former lineage predicting the latter one and the latter lineage predicting the former one'. $*P < 0.05$; $**P < 0.01$; n.s., not significant.

DISCUSSION

Lineage diversification and biogeography

We used a multilocus approach to study the phylogeography of two East Asian babblers, and the nucleotide diversities in 10 anonymous nuclear loci (0.003–0.02 in both species) were comparable to those of Australian red-backed fairy wrens (0.003–0.046; Lee & Edwards, 2008), but slightly higher than those of Atlantic forest antbirds (0.001–0.014; Amaral *et al.*, 2013), European flycatchers (0–0.008; Primmer *et al.*, 2002) and North American chickadees (0–0.002; Harris *et al.*, 2013). The nucleotide diversity of the mtDNA of the two babblers was 0.05 and 0.03 for *A. morrisonia* and *S. ruficeps*, respectively, which was generally higher than that of red-backed fairy wrens (0.013; Lee & Edwards, 2008) and Atlantic forest antbirds (0.003; Amaral *et al.*, 2013).

The mtDNA analyses revealed a geographical structure that is generally congruent with that previously reported for both *A. morrisonia* and *S. ruficeps* (Song *et al.*, 2009; Liu *et al.*, 2012). In both species, the mtDNA analyses supported a reciprocal monophyly for three major lineages: a Taiwan lineage (consisting of individuals from Taiwan, Hainan and east coastal China in *A. morrisonia* and individuals from Taiwan only in *S. ruficeps*), a Southwest Mountain lineage (consisting of individuals from the Yunnan and Sichuan locality groups in *A. morrisonia* and individuals from the Yunnan and Tibet locality groups in *S. ruficeps*), and a Central China lineage (consisting of individuals from the Guangxi and Central China locality groups in *A. morrisonia* and individuals from the Central China, Hainan and Fujian locality groups in *S. ruficeps*). The nDNA analyses also identified these three genetic lineages in the two species of babblers, although with differences in the positions in the trees for the Hainan and east coastal China populations.

Not only are the genetic diversification patterns of the two babbler species similar, the timing of the divergence among the three genetic lineages is also congruent between the species. The divergence times estimated through the coalescent simulations in ABC suggest that the three lineages of both species diversified during the late Pliocene. Both the uplift of the mountains of Southwest China and the formation of the island of Taiwan seem to have driven diversification in *A. morrisonia* and *S. ruficeps*. These species were once widespread in the East Asia, but their distributions became fragmented following geological changes in the region during the Pliocene.

The role of the straits barrier in diversification

Taiwan is a mountainous island situated 230 km away from the mainland. Proto-Taiwan began to form during the late

Table 7 Index of divergence (*D*) from phylogeny-based spatial evolutionary and ecological vicariance analysis (SEEVA) evaluation of *Alcippe morrisonia* and *Stachyridopsis ruficeps* using environmental variables. TW, Taiwan lineage; SM, Southwest Mountain lineage; CC, central China lineage.

Species	Phylogenetic node	Elevation	Vegetation	Temperature annual range	Maximum temperature warmest month	Minimum temperature coldest month	Annual mean temperature	Annual precipitation	Precipitation seasonality	Precipitation of wettest month	Precipitation of driest month
Alcippe morrisonia	TW vs. SM and CC	0.24	**1***	**0.74***	**0.22**	0.47	0.40	0.47	0.46	**0.83***	0.41
	SM vs. CC	0.95*	0.4*	0.67*	0.96*	0.42*	0.95*	0.94*	0.48*	0.65*	0.29
Stachyridopsis ruficeps	TW vs. SM and CC	0.24	**1***	**0.75***	0.37	0.33	0.28	0.9*	0.34	0.9*	0.36
	SM vs. CC	0.94*	0.88*	0.56*	**1***	0.67*	0.92*	0.48*	0.58*	0.56*	0.47

Features with significant *D*-values > 0.75 are listed in bold face.
*Nodes showing significant differences between sister groups using a Bonferroni criterion of $P \leq 0.025$.

Miocene (*c.* 9 Ma) as a result of the tectonic collision of the Luzon arc with the Eurasian margin. The mountains on the island continued to undergo uplift during the Pliocene until *c.* 3 Ma (Sibuet & Hsu, 2004). As new habitats formed in the Pliocene, the island was colonized by different organisms. The founders adapted to the new environment, and the long geographical isolation from their mainland ancestral populations has resulted in the high degree of avian endemism observed today (Lei *et al.*, 2003a,b; Song *et al.*, 2009; Liu *et al.*, 2012). Both *A. morrisonia* and *S. ruficeps* include populations that have been isolated in Taiwan for a long period of time, possibly soon after the formation of the Taiwan Strait in the Pliocene.

In *A. morrisonia*, there is indication of limited gene flow between populations on Taiwan and on the mainland. This can be detected in the mtDNA tree, in which the Taiwan population groups with two populations from the Central China lineage (Fujian and Hainan locality groups). No such connection with the mainland populations can be observed in the nDNA analyses. A similar topological incongruence between nuclear and mitochondrial gene trees has previously been reported in *Parus monticolus* (Wang *et al.*, 2013). Deep divergence between populations in terms of their nDNA lineages combined with evidence of gene flow in mtDNA has often been interpreted as resulting from secondary contact between previously isolated genetic lineages (e.g. Ballard, 2000; Redenbach & Taylor, 2002). In the case of *A. morrisonia* (and *P. monticolus*), we suspect that dispersal may have occurred during the Pleistocene glaciations when the sea level dropped sufficiently to create a land bridge between Taiwan and the mainland. Limited gene flow may be traced through the more rapidly mutating mtDNA, but may not be observed in the nDNA probably because too few loci were analysed. Alternatively, the differences in the signals of gene flow may be explained by a brief period of migration occurring a long time ago. Subsequent gene flow ceased, leaving behind some mtDNA signatures due to maternal inheritance, but the signal was eroded in the nuclear genes due to extensive backcrossing. With more sampled nuclear loci, such as genome-wide SNP loci, and more sophisticated coalescent modelling, we may expect to detect some evidence of gene flow in nuclear genes between the island of Taiwan and mainland populations.

The role of mountain barriers in diversification

Mountainous areas play a key role in avian speciation and diversification because their topographic complexity can lead to ecological stratification and heterogeneity of environment (Fjeldså *et al.*, 2012). Although the uplift of the mountains of Southwest China had already begun in the Miocene, the most intensive tectonic activity occurred in the Pliocene, resulting in most mountains undergoing uplift to over 4000 m a.s.l. (Quade *et al.*, 1989; Webb & Bartlein, 1992). Today, the mountains of Southwest China are characterized by parallel mountain ridges reaching elevations of over
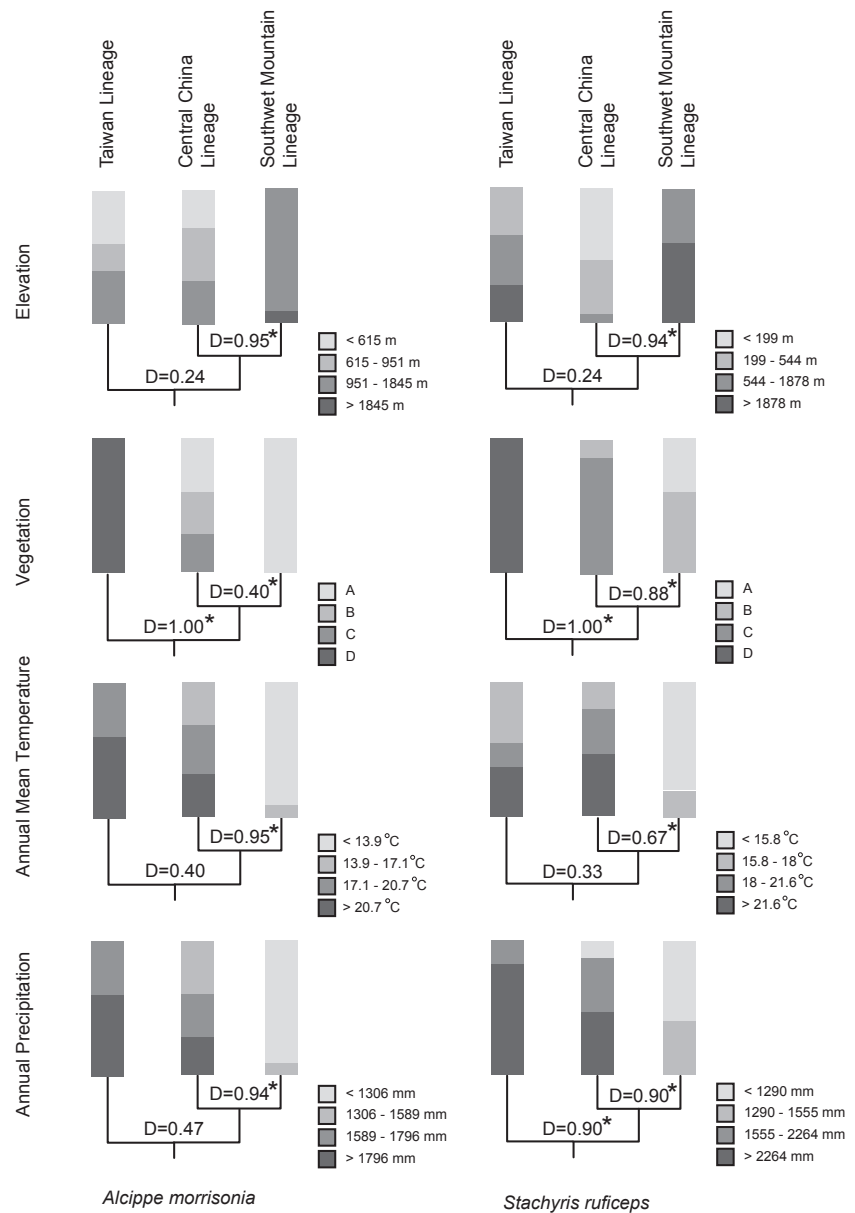
Figure 3 The results of the spatial evolutionary and ecological vicariance analysis (SEEVA) of *Alcippe morrisonia* and *Stachyridopsis ruficeps* using elevation, vegetation, annual mean temperature and annual precipitation coded as four qualitative or quantitative section states (see Materials and Methods for details). The total height of each histogram bar equals 100% of the observations for each lineage, and the greyscale of the histograms represents the four different states. Vegetation: A, plateau evergreen forest; B, mixed forest conifer forest; C, island monsoon rain forest; D, subtropical evergreen forest.

5000 m a.s.l. and elevational differences from valleys to mountain tops that often exceed 2000 m a.s.l. This extreme topographical relief has created dramatic ecological stratification, resulting in geographical isolation for many organisms (Qu *et al.*, 2011, 2014). This situation is evident in *A. morrisonia* and *S. ruficeps*, for which both nuclear and mitochondrial data suggest that the populations in the mountains of Southwest China began to diverge from other populations in Central and South China in the late Pliocene. Furthermore, the mitochondrial phylogenetic trees revealed substructures within the Southwest Mountain lineages (i.e. the Yunnan and Sichuan locality groups in *A. morrisonia* and Yunnan and Tibet locality groups in *S. ruficeps*). Similar endemic genetic lineages and substructures have been observed in *Parus major*, *P. monticolus* and *Aegithalos concinnus* in the mountains of Southwest China (Zhao *et al.*, 2012; Wang *et al.*, 2013). In all of these cases, the mountains of South-

west China have acted as geographical barriers preventing gene flow between populations within and outside of the mountainous region, leading to long-term isolation and *in situ* diversification (Qu *et al.*, 2014).

In many ways, the evolutionary patterns of long-term isolation and *in situ* diversification observed in the mountains of Southwest China are typical of what can be found in an archipelago of islands. In fact, the level of lineage diversification in this region is even higher than that found on the island of Taiwan. Isolated ecosystems, such as mountaintops and mountain systems, have been shown to exhibit island-like properties (Masta, 2000; Smith & Farrell, 2005). In the mountains of Southwest China, specific subregions and mountain systems have served as islands where organisms have been isolated since the Pliocene, which may explain the extraordinarily high number of endemic species and genera found in this region (Lei *et al.*, 2003a,b).

The role of ecological divergence in diversification

The genetic diversification in both species of babblers might also have been driven by ecological divergence given the large differences in ecological niche utilization between populations in the three main lineages. In Taiwan, both species mostly inhabit warm and humid mountain rain forests at elevations between 200 and 1900 m a.s.l. In contrast, in the mountains of Southwest China, *A. morrisonia* and *S. ruficeps* occur at elevations above 2000 m a.s.l and inhabit evergreen, broadleaf and conifer forests. These habitats are mostly dry and cold and exhibit little precipitation during the year. The suitable habitats inhabited by the Central China and Taiwan lineages are much lower in elevation than those in the Southwest Mountain lineages. For most environmental variables, the Central China habitats show an intermediate position between those in the mountains of Southwest China and the island of Taiwan. It is thus reasonable to assume that the climatic differences between lineage-specific niches might have placed ecological constraints on these lineages because each would be adapted to the local conditions. The genetic differentiation resulting from the geographical isolation could be further reinforced and accumulated due to ecological divergence over time. However, to clarify how phylogeographical lineages of the two babblers adapted to local ecological niches, we still need to further explore the genetic evidence from the function-related protein-coding genes.

Phylogeographical lineages and the conservation of genetic endemism

Endemic species richness and diversity are often used to develop and evaluate conservation policies (Mace, 2004). Genetic endemism, which is the consequence of long-term isolation of the intraspecific lineages, should be considered in the design of conservation measures. The phylogeographical lineages preserve the historical components of biodiversity and maintain the potential for species to adapt to environmental changes (D'Amen *et al.*, 2012). For example, although endemic species richness analysis has identified the island of Taiwan and mountains of Southwest China as centres of endemic avian species (Lei *et al.*, 2003a,b), investigation of the phylogeography of *A. morrisonia* and *S. ruficeps* revealed that in both species the major phylogeographical lineages have responded differently to environmental changes in these two regions. For the lineage inhabiting the montane areas in the mountains of Southwest China, the complex topography of the regions has provided enough suitable habitats for isolated populations to persist throughout the Pleistocene (Qu *et al.*, 2014). During this time period, genetic endemism developed and persisted in the Southwest Mountain lineage of *A. morrisonia*. In contrast, the low sea levels during the Pleistocene glaciations allowed individuals belonging to the previously isolated Taiwan lineage to disperse to the mainland. This resulted in genetic admixture between the phylogeographical lineages of Taiwan and Central China and obscured the genetic endemism of the Taiwan lineage. The different responses to habitat changes in the Pleistocene have resulted in the occurrence of a greater number of old endemics and higher genetic diversification in the mountains of Southwest China than on the island of Taiwan. This observation should be taken into consideration when developing future conservation measures to preserve avian endemism in East Asia.

ACKNOWLEDGEMENTS

REFERENCES

Amaral, F.R., Albers, P.K., Ewards, S.V. & Miyaki, C.Y. (2013) Multilocus tests of Pleistocene refugia and ancient divergence in a pair of Atlantic forest antbirds (*Myrmeciza*). *Molecular Ecology*, **22**, 3996–4013.

Ballard, J.W. (2000) Comparative genome of mitochondrial DNA in *Drosophila simulans*. *Journal of Molecular Evolution*, **51**, 64–75.

Carstens, B.C. & Dewey, T.A. (2010) Species delimitation using a combined coalescent and information-theoretic approach: an example from North American *Myotis* bats. *Systematic Biology*, **59**, 400–414.

Cheng, T.H., Long, Z.Y. & Zheng, B.L. (1982) *Fauna Sinica: Aves*, Vol. 11, *Passeriformes, Muscicapidae II Timaliinae*. Science Press, Beijing (in Chinese).

Cornuet, J.M., Santos, F., Beaumont, M.A., Robert, C.R., Marin, J.M., Balding, D.J., Guillemaud, T. & Estoup, A. (2008) Inferring population history with *DIY ABC*: a user-friendly approach to approximate Bayesian computation. *Bioinformatics*, **24**, 2713–2719.

D'Amen, M., Zimmermann, N.E. & Pearman, P.B. (2012) Conservation of phylogeographic lineages under climate change. *Global Ecology and Biogeography*, **22**, 93–104.

Drummond, A.J. & Rambaut, A. (2007) BEAST: Bayesian evolutionary analysis by sampling trees. *BMC Evolutionary Biology*, **7**, 214.

Evanno, G., Regnaut, S. & Goudet, J. (2005) Detecting the number of clusters of individuals using the software STRUCTURE: a simulation study. *Molecular Ecology*, **14**, 2611–2620.

Fjeldså, J., Bowie, R.C.K. & Rahbek, C. (2012) The role of mountain ranges in the diversification of birds. *Annual Review of Ecology, Evolution, and Systematics*, **43**, 249–256.

Gao, B., Qu, Y.H., Song, G., Liu, H.T. & Lei, F.M. (2012) Anonymous single-copy nuclear DNA (scnDNA) markers

for Grey-cheeked Fulvetta (*Alcippe morrisonia*) and Rufous-capped babblers (*Stachyridopsis ruficeps*). *Conservation Genetic Resource*, **4**, 777–781.

Harris, R.B., Carling, M.D. & Lovette, I.J. (2013) The influence of sampling design on species tree inference: a new relationship for the New World chickadees (Aves: Poecile). *Evolution*, **68**, 501–513.

Hijmans, R.J., Cameron, S.E., Parra, J.L., Jones, P.G. & Jarvis, A. (2005) Very high resolution interpolated climate surfaces for global land areas. *International Journal of Climatology*, **25**, 1965–1978.

Kass, R.E. & Raftery, A.E. (1995) Bayes factors. *Journal of the American Statistical Association*, **90**, 773–795.

Kuhner, M., Yamato, J. & Felsenstein, J. (1998) Maximum likelihood estimation of population growth rates based on the coalescent. *Genetics*, **149**, 429–434.

Lee, J.Y. & Edwards, S.V. (2008) Divergence across Australia's Carpentarian barrier: statistical phylogeography of the red-backed fairy wren (*Malurus melanocephalus*). *Evolution*, **62**, 3117–3134.

Lei, F.M., Qu, Y.H., Lu, J.L., Liu, Y. & Yin, Z.H. (2003a) Conservation on diversity and distribution patterns of endemic birds in China. *Biodiversity and Conservation*, **12**, 239–254.

Lei, F.M., Qu, Y.H., Tang, Q.Q. & An, S.C. (2003b) Priorities for the conservation of avian biodiversity in China based on the distribution patterns of endemic bird genera. *Biodiversity and Conservation*, **12**, 2487–2501.

Lei, F.M., Qu, Y.H. & Song, G. (2014) Species diversification and phylogeographical patterns of birds in response to the uplift of the Qinghai-Tibet Plateau and Quaternary glaciations. *Current Zoology*, **60**, 149–161.

Li, S.H., Yeung, C.K.L., Feinstein, J., Han, L.X., Le, H.M., Wang, C.X. & Ding, P. (2009) Sailing through the Late Pleistocene: unusual historical demography of an East Asian endemic, the Chinese Hwamei (*Leucodioptron canorum canorum*), during the last glacial period. *Molecular Ecology*, **18**, 622–633.

Liu, L. & Pearl, D.K. (2007) Species trees from gene trees: reconstructing Bayesian posterior distributions of species phylogeny using estimated gene tree distributions. *Systematic Biology*, **56**, 504–505.

Liu, H.T., Wang, W.J., Song, G., Qu, Y.H., Li, S.H., Fjeldså, J. & Lei, F.M. (2012) Interpreting the process behind endemism in China by integrating the phylogeography and ecological niche models of the *Stachyridopsis ruficeps*. *PLoS ONE*, **7**, e46761.

Mace, G.M. (2004) The role of taxonomy in species conservation. *Philosophical Transactions of the Royal Society B: Biological Sciences*, **359**, 711–719.

Maddison, W.P. & Maddison, D.R. (2009) *Mesquite: a modular system for evolutionary analysis*. Version 2.5. Available at: http://mesquiteproject.org/.

Masta, S.E. (2000) Phylogeography of the jumping spider *Habronattus pugillis* (Araneae: Salticidae): recent vicariance of sky island populations? *Evolution*, **54**, 1699–1711.

Päckert, M., Martens, J., Sun, Y-H., Severinghaus, L.L., Nazarenko, A.A., Ting, J., Topfer, T. & Tietze, D.T. (2012) Horizontal and elevational phylogeographic patterns of Himalayan and Southeast Asian forest passerines (Aves: Passeriformes). *Journal of Biogeography*, **39**, 556–573.

Posada, D. & Crandall, K.A. (1998) Modeltest: testing the model of DNA substitution. *Bioinformatics*, **14**, 817–818.

Primmer, C.R., Borge, T., Lindell, J. & Saetre, G.P. (2002) Single-nucleotide polymorphism characterization in species with limited available sequence information: high nucleotide diversity revealed in the avian genome. *Molecular Ecology*, **11**, 603–612.

Pritchard, J.K., Stephens, M. & Donnelly, P. (2000) Inference of population structure using multilocus genotype data. *Genetics*, **55**, 945–959.

Qu, Y.H., Luo, X., Zhang, R.Y., Song, G., Zou, F.S. & Lei, F.M. (2011) Lineage diversification and historical demography of a montane bird *Garrulax elliotii* – implications for the Pleistocene evolutionary history of the eastern Himalayas. *BMC Evolutionary Biology*, **11**, 174.

Qu, Y.H., Ericson, P.G.P., Quan, Q., Song, G., Zhang, R.Y., Gao, B. & Lei, F.M. (2014) Long-term isolation and stability explain high genetic diversity in the Eastern Himalaya. *Molecular Ecology*, **23**, 807–720.

Quade, J., Cerling, T.E. & Bowman, J.R. (1989) Development of Asian monsoon revealed by marked ecological shift during the latest Miocene in northern Pakistan. *Nature*, **342**, 163.

Rambaut, A. & Drummond, A.J. (2007) *Tracer v1.5*. Available at: http://beast.bio.ed.ac.uk/software/tracer/.

Redenbach, Z. & Taylor, E.B. (2002) Evidence for historical introgression along a contact zone between two species of charr (Pisces: Salmonidae) in northwestern North America. *Evolution*, **56**, 1021–1035.

Ronquist, F. & Huelsenbeck, J.P. (2003) MRBAYES 3: Bayesian phylogenetic inference under mixed models. *Bioinformatics*, **19**, 1572–1574.

Schoener, T.W. (1968) The *Anolis* lizards of Bimini: resource partitioning in a complex fauna. *Ecology*, **49**, 704–726.

Sibuet, J.C. & Hsu, S.K. (2004) How was Taiwan created? *Tectonophysics*, **379**, 159–181.

Smith, C.I. & Farrell, B.D. (2005) Phylogeography of the longhorn cactus beetle *Moneilema appressum* LeConte (Coleoptera: Cerambycidae): was the differentiation of the Madrean sky islands driven by Pleistocene climate changes? *Molecular Ecology*, **14**, 3049–3065.

Song, G., Qu, Y.H., Yin, Z.H., Li, S.H., Liu, N.F. & Lei, F.M. (2009) Phylogeography of the *Alcippe morrisonia* (Aves: Timaliidae): long population history beyond late Pleistocene glaciations. *BMC Evolutionary Biology*, **9**, 143.

Stattersfield, A.J., Crosby, M.J., Long, A.J. & Wege, D.C. (1998) *Endemic bird areas of the world: priorities for biodiversity conservation*. BirdLife International, Cambridge, UK.

Struwe, L., Smouse, P.R., Heiberg, E., Haag, S. & Lathrop, R.G. (2011) Spatial evolutionary and ecological vicariance analysis (SEEVA), a novel approach to biogeography and

speciation research, with an example from Brazilian Gentianaceae. *Journal of Biogeography*, **38**, 1841–1854.

Voris, H.K. (2000) Maps of Pleistocene sea levels in Southeast Asia: shorelines, river systems and time durations. *Journal of Biogeography*, **27**, 1153–1167.

Wang, W.J., McKay, B.D., Dai, C.Y., Zhao, N., Zhang, R.Y., Qu, Y.H., Song, G., Li, S.H., Liang, W., Yang, X.J., Pasquet, E. & Lei, F.M. (2013) Glacial expansion and diversification of an East Asian montane bird, the green-backed tit (*Parus monticolus*). *Journal of Biogeography*, **40**, 1156–1169.

Warren, D.L., Glor, R.E. & Turelli, M. (2008) Environmental niche equivalency versus conservatism: quantitative approaches to niche evolution. *Evolution*, **62**, 2868–2883.

Webb, T., III & Bartlein, P.J. (1992) Global changes during the last 3 million years: climatic controls and biotic responses. *Annual Review of Ecology and Systematics*, **23**, 141–173.

Yang, Z. & Rannala, B. (2010) Bayesian species delimitation using multilocus sequence data. *Proceedings of the National Academy of Sciences USA*, **107**, 9264–9269.

Yu, G., Chen, X., Ni, J. *et al.* (2000) Palaeovegetation of China: a pollen data-based synthesis for the mid-Holocene and last glacial maximum. *Journal of Biogeography*, **27**, 635–664.

Zhao, N., Dai, C.Y., Wang, W.J., Zhang, R.Y., Qu, Y.H., Song, G., Chen, K., Yang, X.J., Zou, F.S. & Lei, F.M. (2012) Pleistocene climate changes shaped the divergence and demography of Asian populations of the great tit *Parus major*: evidence from phylogeographic analysis and ecological niche models. *Journal of Avian Biology*, **43**, 297–310.

SUPPORTING INFORMATION

Additional Supporting Information may be found in the online version of this article:

Appendix S1 The GenBank accession numbers of all sequences of *Alcippe morrisonia* and *Stachyridopsis ruficeps* used in the study.

Appendix S2 Coalescent simulation models used in the approximate Bayesian computation (ABC) analyses.

Appendix S3 Bayesian gene trees of 10 nuclear loci constructed in MrBayes.

DATA ACCESSIBILITY

Sample information and GenBank accession numbers for all sequenced individuals are given in Appendix S1 in the Supporting Information.

BIOSKETCH

Yanhua Qu is a professor and senior researcher at the Ornithological Research Group, Institute of Zoology, Chinese Academy of Sciences. Her research interests focus on the genetic diversification and speciation of birds in China.

Author contributions: Y.H.Q. and F.M.L. conceived and designed the study. G.S. and B.G. performed laboratory work. Q.Q. performed the ecological niche modelling work. Y.H.Q. and F.M.L. drafted the paper. P.E participated in the analyses and finalized the manuscript together with Y.H.Q. and F.M.L.

Editor: Brett Riddle